

Fig. 11. The percent relative error in (a) the Gaussian curvature and (b) the mean curvature as a function of tuning constant for the synthetic patch. Solid curve: clean. Dashed curve: with normal noise. Dotted curve: normal and an outlier. Dot-dash curve: with outliers. (c) Real spherical patch.

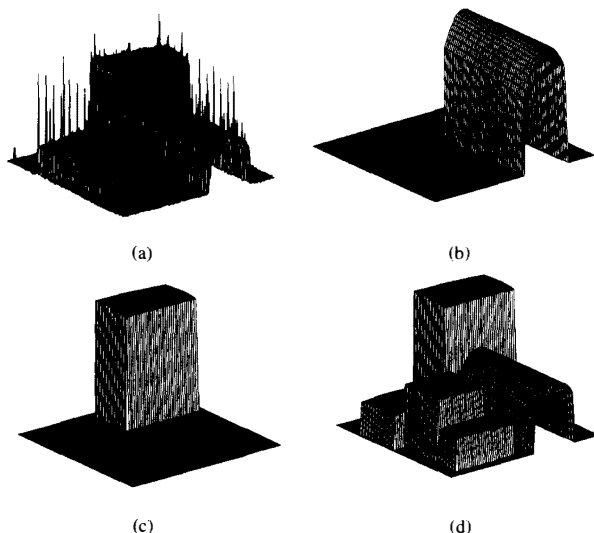


Fig. 12. Real range image of a jumble of packages. (a) Raw data including noise and outliers. Reconstructed biquadratic surfaces to maximal rectangular footprints. (b) Cylinder. (c) Rectangular box. (d) All objects.

- [9] R. M. Haralick, "Computer vision theory: The lack thereof," *Comput. Vision, Graphics, Image Process.*, vol. 36, pp. 372-386, 1986.
- [10] W. Forstner, "Reliability analysis of parameter estimation in linear models with application to mensuration problems in computer vision," *Comput. Vision, Graphics, Image Process.*, vol. 40, pp. 273-310, 1987.
- [11] P. J. Besl, J. B. Birch, and L. T. Watson, "Robust window operators," in *Proc. Int. Conf. Comput. Vision (ICCV '88)*, 1988.
- [12] R. M. Haralick, H. Joo, C. Lee, X. Zhuang, and V. V. M. Kim, "Pose estimation from corresponding point data," *IEEE Trans. Syst. Man Cybern.*, vol. 19, pp. 1426-1446, 1989.
- [13] D. S. Chen, "A data-driven intermediate level feature extraction algorithm," *IEEE Trans. Pattern Anal. Machine Intell.*, vol. 11, no. 7, pp. 749-758, 1988.

- [14] D. Y. Kim, J. J. Kim, P. Meer, D. Mintz, and A. Rosenfeld, "Robust computer vision: A least-median of squares based approach," in *Proc. DARPA Image Understanding Workshop*, 1989.
- [15] S. S. Sinha and B. G. Schunck, "A two-stage algorithm for discontinuity-preserving surface reconstruction," *IEEE Trans. Pattern Anal. Machine Intell.*, vol. 14, pp. 36-55, Jan. 1992.
- [16] A. E. Beaton and J. W. Tukey, "The fitting of power series, meaning polynomials, illustrated on band-spectroscopic data," *Technometrics*, vol. 16, pp. 147-185, May 1974.
- [17] D. Andrews, P. Bickel, F. Hampel, P. Huber, W. Rogers, and J. Tukey, *Robust Estimates of Location: Survey and Advances*. Princeton: Princeton University Press, 1972.
- [18] P. W. Holland and R. E. Welsch, "Robust regression using iteratively reweighted least-squares," *Commun. Statist.-Theor. Meth.*, vol. A6, no. 9, pp. 813-827, 1977.
- [19] C. Goodall, "M-estimator of location: An outline of the theory," in *Understanding Robust and Exploratory Data Analysis*, D. C. Hoaglin, F. Mosteller, and J. W. Tukey, Eds. New York: 1983, pp. 339-403.

## Dynamic Control of a Manipulator with Passive Joints in Operational Space

Hirohiko Arai, Kazuo Tanie, and Susumu Tachi

**Abstract**—We present a method to control a manipulator with passive joints, which have no actuators, in operational space. The equation of motion is described in terms of operational coordinates. The coordinates are separated into *active* and *passive* components. The acceleration of the active components can be arbitrarily adjusted by using the coupling characteristics of manipulator dynamics. This method is also extended to path tracking control of a manipulator with passive joints. A desired path is geometrically specified in operational space. The position of the manipulator is controlled to follow the path. In this method, a *path coordinate system* based on the path is defined in operational space. The path coordinates consist of a component parallel to the path and components normal to the path. The acceleration of the components normal to the path is controlled according to feedback based on tracking error by using the dynamic coupling among the components. This in turn keeps the manipulator on the path. The effectiveness of the method is verified by experiments using a two-degree-of-freedom manipulator with a passive joint.

### I. INTRODUCTION

The number of degrees of freedom of a conventional manipulator is equal to the number of joint actuators. Since the mass of the actuator of a serial-type manipulator is a load for the next actuator, the size of the actuator should increase rapidly from the wrist joint to the base joint. As a result, the base joint must be equipped with a huge actuator compared to the load of the manipulator. In order to decrease the weight, cost, and energy consumption of a manipulator, various methods have been proposed for controlling a manipulator that has more degrees of freedom than actuators [1]. However, these methods

Manuscript received August 8, 1991; revised April 17, 1992. A portion of this work was presented at the 1991 IEEE International Conference on Robotics and Automation, Sacramento, CA, April 9-11, 1991, and at the 1991 IEEE/RSJ International Workshop on Intelligent Robots and Systems, Osaka, Japan, November 2-4, 1991.

H. Arai and K. Tanie are with the Mechanical Engineering Laboratory, AIST, MITI, 1-2 Namiki, Tsukuba, Ibaraki 305, Japan.

S. Tachi is with RCAST, The University of Tokyo, 4-6-1 Komaba, Meguro-ku, Tokyo 153, Japan.

IEEE Log Number 9205078.

require special mechanisms in addition to basic links and joints. In this paper, a method is presented for controlling a manipulator that has more joints than actuators without using additional mechanisms except joint brakes.

The dynamics of a manipulator have nonlinear and coupling characteristics. When each joint is controlled by a local linear feedback loop, these factors result in disturbances. The elimination of such dynamic disturbances has been one of the major problems in manipulator control [2]–[4]. A design theory for a manipulator with neither nonlinearities nor dynamic coupling has also been proposed [5]. However, the effects of these disturbances are available to drive a joint that in itself does not have an actuator. Such dynamic characteristics are actively used in human handling tasks. For example, when a heavy load is handled, all the muscles of the human arm are not necessarily used. Some joints, e.g., wrist joints, are kept free, and the inertia of the load is utilized effectively. Such a *dynamic skill* will also be significant for robot control. Some robot control schemes that utilize dynamic coupling effects have previously been proposed [6], [7].

As a means of controlling a manipulator with more joints than actuators without using additional mechanisms, we propose controlling passive joints by using dynamic coupling [8]. We developed an algorithm for point-to-point control of the manipulator and applied it to a two-degree-of-freedom (2-DOF) manipulator [9]. In this method, a manipulator is composed of two types of joints: active and passive. Each active joint consists of an actuator and a position sensor (e.g., an encoder). Each passive joint consists of a holding brake and a position sensor. When the brakes of the passive joints are engaged, the active joints can be controlled without affecting the state of the passive joints. When the brakes are released, the passive joints can rotate freely. The motion of the active joints generates acceleration of the passive joints via the coupling characteristics of manipulator dynamics. The passive joints can be controlled indirectly in this manner. The total position of the manipulator is controlled by combining these two control modes. Jain and Rodriguez independently proposed a similar technique to control a manipulator with passive hinges. They also developed an efficient dynamics algorithm using spatial operator algebra [10].

When some of the joint actuators of a manipulator are exchanged for holding brakes with this method, we can build a lightweight, energy-saving, low-cost manipulator. We can take advantage of these merits by applying the method to simple assembly robots, control of redundant manipulators, etc. Space applications (e.g., space manipulators, expansion of space structure) may be feasible. This method can also be applied to failure recovery control of a manipulator [11].

Control with the passive joints released is an essential part of this method. In [8] and [9], we controlled the manipulator in joint space. In this approach, a desired trajectory is assigned to the passive joints, and the motion and torque of the active joints is calculated to realize the desired motion of the passive joints. The motion of the active joints is determined by the desired trajectory of the passive joints and the dynamic coupling among the joints. Consequently, the motion of the tip of the manipulator cannot be prescribed. However, the position of the tip in operational space, e.g., Cartesian space, is usually important for practical manipulator tasks. It is necessary to control the path along which the tip moves if the manipulator is to avoid collision with an obstacle.

In this paper, we extend our previous work on control in joint space to control in operational space. In Section II, the control scheme in operational space is presented. The equation of motion is represented in terms of operational coordinates. The operational coordinates are separated into *active components* and *passive components*. The

desired acceleration is generated at the active components, which are equal in number to the active joints, by using dynamic coupling among the components. This method is extended to path-tracking control of a manipulator with passive joints. A desired path is geometrically specified in operational space. The tip position of the manipulator is controlled to follow the desired path. In Section III, *path coordinates* are defined as a kind of operational coordinate system based on the desired path. The path coordinates consist of a component parallel to the desired path and components normal to the desired path. In Section IV, a method for path-tracking control is described. The acceleration of the components normal to the desired path is controlled by using the dynamic coupling among components. This in turn keeps the manipulator on the desired path. In Section V, the effectiveness of the proposed methods is demonstrated by experiments using a 2-DOF manipulator with a passive joint.

## II. CONTROL IN OPERATIONAL SPACE

### A. Equation of Motion with Operational Coordinates

An  $n$ -DOF manipulator is considered here. The operational space is assumed to be  $n$ -dimensional. We assume  $r$  DOF of the manipulator are active joints. The remaining  $n - r$  DOF are passive joints with holding brakes instead of actuators.

The equation of motion of the manipulator in joint space can be written as

$$\mathbf{M}(\theta)\ddot{\theta} + \mathbf{b}(\theta, \dot{\theta}) = \mathbf{u} \quad (1)$$

where

$$\mathbf{b}(\theta, \dot{\theta}) = \mathbf{h}(\theta, \dot{\theta}) + \mathbf{\Gamma}\dot{\theta} + \mathbf{g}(\theta)$$

and

$\theta \in \mathbb{R}^n$	joint angle vector,
$\mathbf{u} \in \mathbb{R}^n$	joint torque vector,
$\mathbf{g}(\theta) \in \mathbb{R}^n$	gravity torque vector,
$\mathbf{h}(\theta, \dot{\theta}) \in \mathbb{R}^n$	Coriolis and centrifugal torque vector,
$\mathbf{M}(\theta) \in \mathbb{R}^{n \times n}$	inertia matrix,
$\mathbf{\Gamma} \in \mathbb{R}^{n \times n}$	viscous friction matrix.

The elements of  $\mathbf{u}$  are rearranged as

$$\mathbf{u} = [\tau^T \quad \mathbf{0}]^T. \quad (2)$$

$\tau \in \mathbb{R}^r$  is the torque of the active joints, and the torque of the passive joints is zero. Accordingly,  $\mathbf{M}$  and  $\mathbf{b}$  are also rearranged and partitioned as follows:

$$\mathbf{M} = \begin{bmatrix} \mathbf{M}_a \\ \mathbf{M}_b \end{bmatrix}, \quad \mathbf{b} = \begin{bmatrix} \mathbf{b}_a \\ \mathbf{b}_p \end{bmatrix} \quad (3)$$

where  $\mathbf{M}_a \in \mathbb{R}^{r \times n}$ ,  $\mathbf{M}_b \in \mathbb{R}^{(n-r) \times n}$ ,  $\mathbf{b}_a \in \mathbb{R}^r$ , and  $\mathbf{b}_p \in \mathbb{R}^{n-r}$ .

The equation of motion of the manipulator is rewritten in terms of operational coordinates  $\mathbf{p} \in \mathbb{R}^n$ . We assume that the operational coordinates and the joint coordinates are related as follows:

$$\dot{\mathbf{p}} = \mathbf{J}\dot{\theta} \quad (4)$$

where  $\mathbf{J}(\theta) \in \mathbb{R}^{n \times n}$  is a Jacobian matrix. When (4) is differentiated with respect to time, we obtain

$$\ddot{\mathbf{p}} = \mathbf{J}\ddot{\theta} + \dot{\mathbf{J}}\dot{\theta} \quad (5)$$

If  $\mathbf{J}$  is nonsingular

$$\ddot{\theta} = \mathbf{J}^{-1}(\ddot{\mathbf{p}} - \dot{\mathbf{J}}\dot{\theta}). \quad (6)$$

Note that the manipulator has  $n$  DOF and is nonredundant. When the manipulator is redundant, matrix  $\mathbf{J}$  is not invertible. One way to

invert  $\mathbf{J}$  is the *extended Jacobian method* [12], in which auxiliary coordinates are added to the operational coordinates so that  $\mathbf{J}$  can be inverted.

The  $r$  components of the operational coordinates, which should be controlled, are chosen and grouped as  $\mathbf{x}$ . The remaining components are grouped as  $\mathbf{y}$ . Here,  $\mathbf{p}$  and  $\mathbf{H} \equiv \mathbf{J}^{-1}$  are rearranged and partitioned as follows:

$$\mathbf{p} = \begin{bmatrix} \mathbf{x} \\ \mathbf{y} \end{bmatrix}, \quad \mathbf{H} = [\mathbf{H}_a \quad \mathbf{H}_p] \quad (7)$$

where  $\mathbf{x} \in \mathbb{R}^r$ ,  $\mathbf{y} \in \mathbb{R}^{n-r}$ ,  $\mathbf{H}_a \in \mathbb{R}^{n \times r}$ , and  $\mathbf{H}_p \in \mathbb{R}^{n \times (n-r)}$ . We define  $\mathbf{x}$  as an *active component* and  $\mathbf{y}$  as a *passive component*. The desired motion is assigned to the active components while the passive components are controlled so as to realize the desired motion of the active components. When (3), (6), and (7) are substituted in (1), we obtain

$$\mathbf{M}_a \mathbf{H}_a \ddot{\mathbf{x}} + \mathbf{M}_a \mathbf{H}_p \ddot{\mathbf{y}} - \mathbf{M}_a \mathbf{H} \dot{\mathbf{J}} \dot{\theta} + \mathbf{b}_a = \boldsymbol{\tau} \quad (8a)$$

$$\mathbf{M}_p \mathbf{H}_a \ddot{\mathbf{x}} + \mathbf{M}_p \mathbf{H}_p \ddot{\mathbf{y}} - \mathbf{M}_p \mathbf{H} \dot{\mathbf{J}} \dot{\theta} + \mathbf{b}_p = \mathbf{0}. \quad (8b)$$

The equation of motion is represented in terms of the active and passive operational coordinates. Moreover, it is divided into (8a), which is related to torque of the active joints, and (8b), which is related to torque of the passive joints.

### B. Control in Operational Space

The desired acceleration can be generated arbitrarily at components equal in number to the active joints. Control of the active components is given priority, and the computed torque method [2] is applied. It prescribes a desired trajectory for the active components and generates the motion of the passive components in order to realize the desired trajectory of the active components.

The desired position  $\mathbf{x}_d$ , velocity  $\dot{\mathbf{x}}_d$ , and acceleration  $\ddot{\mathbf{x}}_d$  of the active components are obtained from the desired trajectory. The following PID control is applied to suppress the tracking error:

$$\ddot{\mathbf{x}}_d = \ddot{\mathbf{x}}_d + \mathbf{K}_v(\dot{\mathbf{x}}_d - \dot{\mathbf{x}}) + \mathbf{K}_p(\mathbf{x}_d - \mathbf{x}) + \mathbf{K}_i \int (\mathbf{x}_d - \mathbf{x}) dt \quad (9)$$

where  $\mathbf{K}_v$ ,  $\mathbf{K}_p$ , and  $\mathbf{K}_i \in \mathbb{R}^{r \times r}$  are the diagonal gain matrices.

When measured values of the joint angle and velocity are substituted in  $\theta$  and  $\dot{\theta}$  of (8a) and (8b), each component of  $\mathbf{M}$ ,  $\mathbf{H}$ ,  $\mathbf{J}$ , and  $\mathbf{b}$  is determined. If  $\ddot{\mathbf{x}}_d$  of (9) is assigned to the acceleration  $\ddot{\mathbf{x}}$  of the active component  $\mathbf{x}$ , (8b) can be considered as a linear equation with regard to  $\ddot{\mathbf{y}}$ . If  $\mathbf{M}_p \mathbf{H}_p \in \mathbb{R}^{(n-r) \times (n-r)}$  is nonsingular (and hence invertible), (8b) can be solved uniquely as

$$\ddot{\mathbf{y}} = (\mathbf{M}_p \mathbf{H}_p)^{-1} (-\mathbf{M}_p \mathbf{H}_a \ddot{\mathbf{x}}_d + \mathbf{M}_p \mathbf{H} \dot{\mathbf{J}} \dot{\theta} - \mathbf{b}_p). \quad (10)$$

The nonsingularities of  $\mathbf{J}$  and  $\mathbf{M}_p \mathbf{H}_p$  are essential for this method. The singularity of  $\mathbf{M}_p \mathbf{H}_p$  (dynamic singularity) will be discussed later.

When (10) is substituted in (8a), the torque  $\boldsymbol{\tau}$  to realize the acceleration  $\ddot{\mathbf{x}}_d$  can be determined.

$$\boldsymbol{\tau} = \{ \mathbf{M}_a - \mathbf{M}_a \mathbf{H}_p (\mathbf{M}_p \mathbf{H}_p)^{-1} \mathbf{M}_p \} (\mathbf{H}_a \ddot{\mathbf{x}}_d - \mathbf{H} \dot{\mathbf{J}} \dot{\theta}) + \mathbf{b}_a - \mathbf{M}_a \mathbf{H}_p (\mathbf{M}_p \mathbf{H}_p)^{-1} \mathbf{b}_p. \quad (11)$$

When we apply this torque  $\boldsymbol{\tau}$  to the active joints, we will obtain the acceleration  $\ddot{\mathbf{x}}_d$ . The active components are guaranteed to converge to the desired values if  $\mathbf{K}_v$ ,  $\mathbf{K}_p$ , and  $\mathbf{K}_i$  are chosen such that all the poles of the feedback system are located in the left-half plane. Fig. 1 represents a block diagram of the control system.

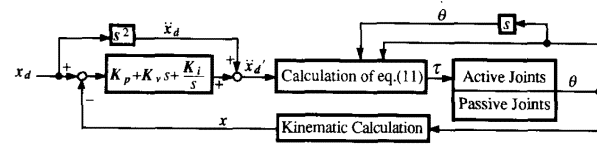


Fig. 1. Control system in operational space.

### C. Function of Brakes

The brakes of the passive joints are used to set up the initial conditions. When the brakes are engaged, the manipulator has  $r$  degrees of freedom. The passive joints are fixed, and the angular velocity is zero. The number of the active components is  $r$ . The active components are represented by a kinematic equation including the angle of the active joints. Therefore, the initial angle and angular velocity of the active joints that realize initial position  $\mathbf{x}_0$  and initial velocity  $\dot{\mathbf{x}}_0$  of the active components can be obtained by inverse kinematics.

The initial conditions of the passive components cannot be set up by the active joints alone. If the initial position of the passive components needs to be set up, it is necessary to use the point-to-point algorithm of [8]. The initial velocity of the passive components is determined by the initial velocity of the active components.

The final conditions of the passive components are determined by the control hysteresis of the active components. Even if the manipulator is at rest in the initial condition and the final velocity of the active components is controlled at zero, the final velocity of the passive components is generally not zero. In the experiments, we forced the passive joints to stop with the brake. In this method, the passive joints cannot stop at an exact angle because of the time delay in the brake operation. It is necessary to switch from operational space control to joint space control and to stop the passive joints before braking if the purpose of the control is positioning.

### D. Dynamic Singularity

The conditions required for this control method are as follows:

- 1) Matrix  $\mathbf{H}$  can be obtained. (Jacobian matrix  $\mathbf{J}$  is invertible.)
- 2) Equation (8b) has a unique solution. ( $\ddot{\mathbf{y}}$  is determined uniquely.)
- 3) In (11),  $\boldsymbol{\tau}$  and  $\ddot{\mathbf{x}}_d$  show one-to-one correspondence.

Condition 1 means that the manipulator must be kinematically nonsingular. Condition 2 is equivalent to the nonsingularity of matrix  $\mathbf{M}_p \mathbf{H}_p$  ( $\det[\mathbf{M}_p \mathbf{H}_p] \neq 0$ ). Condition 3 is the nonsingularity of matrix  $\{ \mathbf{M}_a - \mathbf{M}_a \mathbf{H}_p (\mathbf{M}_p \mathbf{H}_p)^{-1} \mathbf{M}_p \} \mathbf{H}_a$ . Conditions 2 and 3 are mathematically equivalent. The acceleration of the passive components cannot influence the acceleration of the active components in the positions where  $\mathbf{M}_p \mathbf{H}_p$  is singular. The acceleration of the active components is determined by the position and velocity of the manipulator, regardless of the acceleration of the passive components. Therefore, this method is difficult to use near these dynamic singular points.

The condition of dynamic singularity ( $\det[\mathbf{M}_p \mathbf{H}_p] = 0$ ) provides one degree of constraint. For example, when a manipulator has 3 DOF, the dynamic singular points compose a surface. The manipulator cannot pass through this surface in the proposed method. An algorithm to solve this problem is necessary. One way to solve this problem is to use the brakes and fix the passive joints. Another solution is to switch the choice of the active components. The inertia matrix  $\mathbf{M}$  is generally nonsingular. Therefore, the rank of matrix  $\mathbf{M}_p$  is  $n - r$ . Singularity of  $\mathbf{M}_p \mathbf{H}_p$  depends on  $\mathbf{H}_p$ . If the active components are chosen in a different way, the manipulator can pass near the dynamic singular points. (Of course, control of the former active components is compromised in this case.)

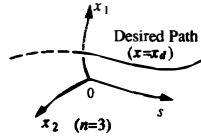


Fig. 2. Path coordinate system.

### III. PATH COORDINATES

In the following sections, a method for path tracking control is presented. A mathematical description of the desired path is considered at first. The desired path is geometrically specified as a continuous curve in operational space. It is not associated with a time variable. In minimum-time trajectory planning problems, this type of path is often parameterized by a path parameter [13]–[15]. The position of a point on the path is represented as a vector function of a scalar parameter. When operational space is  $n$ -dimensional, a point  $q \in \mathbb{R}^n$  on the path is represented as

$$q = q(s), s_0 \leq s \leq s_f \quad (12)$$

where  $s$  is the path parameter.  $q(s_0)$  is the start point of the path and  $q(s_f)$  is the end point.  $s$  can be considered as a distance along the path. Since  $s$  is a scalar, this method can represent a point only on the path itself.

Real-time path tracking control is considered here. If the manipulator deviates from the path due to disturbances, feedback control should force the manipulator to return to the path. Therefore, points not on the path as well as points on the path should be represented. Furthermore, the tracking error should be measured. We propose the concept of *path coordinates* as an extension of the path parameter. A curvilinear coordinate frame is defined in operational space. The coordinates are composed of a component  $s$  along the path and components  $x_1, \dots, x_{n-1}$  normal to  $s$ .  $x_i$  is normal to  $x_j$  if  $i \neq j$ . These coordinates are called path coordinates (Fig. 2). A point  $p \in \mathbb{R}^n$  represented in terms of the path coordinates is

$$p = [x_1, \dots, x_{n-1}, s]^T = [x^T \ s]^T. \quad (13)$$

The desired path is represented as

$$x = x_d(\text{constant}), \quad s_0 \leq s \leq s_f \quad (14)$$

in terms of the path coordinates. The desired path is also represented as

$$q = q([x_d^T \ s]^T), \quad s_0 \leq s \leq s_f \quad (15)$$

in terms of the operational coordinates. Equation (15) can be extended to represent all points in operational space. A point  $q$  in operational space is represented as a vector function of path coordinate  $p$ .

$$q = q(p). \quad (16)$$

Equation (16) represents the coordinate transformation from the path coordinate space to operational space.

*Example:* Operational coordinates: Cartesian coordinates ( $n = 3$ ). Desired path: A circle of radius  $r_0$ , centered at  $[x_0, y_0, z_0]$ , parallel to the  $xy$  plane

$$q(s) = [r_0 \cos(\omega s) + x_0, r_0 \sin(\omega s) + y_0, z_0].$$

Path coordinates: Cylindrical coordinates

$$\begin{aligned} q(p) &= q([x_1, x_2, s]^T) \\ &= [x_1 \cos(\omega s) + x_0, x_1 \sin(\omega s) + y_0, x_2]. \end{aligned}$$

The desired path is represented as

$$x = [x_1, x_2]^T = [r_0, z_0]^T$$

in terms of path coordinates. Note that there exist lots of path coordinate systems for one desired path. In the case of this example, a spherical coordinate that has its origin at the center of the desired path can also be a path coordinate.

### IV. PATH-TRACKING CONTROL

In this section, the path-tracking control scheme is described. The control scheme is based on the path coordinates. First, the equation of motion is represented in terms of the path coordinates. Then the path-tracking control scheme with feedback is proposed. The initial conditions of the desired path are discussed. Path tracking with multiple passive joints is also considered.

#### A. Path-Tracking Control

Both operational space and the path coordinate space are assumed to be  $n$ -dimensional. It is assumed that the manipulator also has  $n$  DOF, and it consists of  $n - 1$  active joints and one passive joint.

We propose a control method in which the manipulator tracks the desired path defined in Section III. In Section II, it was shown that the components equal in number to the active joints can be active components and controllable. The number of active joints of the present manipulator is  $n - 1$ . The number of components of the path coordinates is  $n$ , and the number of components  $x$  normal to the path is  $n - 1$ . Therefore,  $x$  is treated as an active component and  $s$  is treated as a passive component.

From (16), the operational coordinate  $q$  and the path coordinate  $p$  are related as  $q = q(p)$ . The operational coordinate  $q$  is calculated by forward kinematics,  $q = q(\theta)$ . When

$$J_1 = \frac{\partial q}{\partial p}, \quad J_2 = \frac{\partial q}{\partial \theta}, \quad J_1, J_2 \in \mathbb{R}^{n \times n}$$

the Jacobian matrix  $J(\theta) \in \mathbb{R}^{n \times n}$  of path coordinate  $p$  for joint coordinate  $\theta$  is represented as

$$J = \frac{\partial p}{\partial \theta} = J_1^{-1} J_2.$$

Consequently,  $p$  and  $\theta$  are related as

$$\dot{p} = J \dot{\theta}. \quad (17)$$

The equation of motion in joint space is written as

$$M(\theta) \ddot{\theta} + b(\theta, \dot{\theta}) = u. \quad (18)$$

The equation of motion of the manipulator is rewritten in terms of  $p \in \mathbb{R}^n$ . The joint torque vector  $u$  is composed of the active joint torque,  $\tau \in \mathbb{R}^{n-1}$ , and the passive joint torque (= 0).

$$u = [\tau^T \ 0]^T. \quad (19)$$

Then the same procedure as in Section II results in the following equation:

$$M_a H_a \ddot{x} + M_a H_p \ddot{s} - M_a H \dot{J} \dot{\theta} + b_a = \tau \quad (20a)$$

$$M_p H_a \ddot{x} + M_p H_p \ddot{s} - M_p H \dot{J} \dot{\theta} + b_p = 0 \quad (20b)$$

where

$$M = \begin{bmatrix} M_a \\ M_p \end{bmatrix}, \quad b = \begin{bmatrix} b_a \\ b_p \end{bmatrix}, \quad J^{-1} = H = [H_a \ H_p] \quad (21)$$

and  $M_a \in \mathbb{R}^{(n-1) \times n}$ ,  $M_p \in \mathbb{R}^{1 \times n}$ ,  $b_a \in \mathbb{R}^{n-1}$ ,  $b_p \in \mathbb{R}^1$ ,  $H_a \in \mathbb{R}^{n \times (n-1)}$ , and  $H_p \in \mathbb{R}^{n \times 1}$ .

In order to keep the manipulator on the desired path, the  $x$  components normal to the path should remain constant at  $x_d$ . The

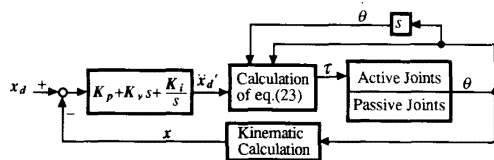


Fig. 3. Path-tracking control system.

acceleration  $\ddot{x}_d$  is generated to adjust  $\mathbf{x}$  to  $\mathbf{x}_d$ . The following PID control is applied:

$$\ddot{x}_d = -K_v \dot{x} + K_p (\mathbf{x}_d - \mathbf{x}) + K_i \int (\mathbf{x}_d - \mathbf{x}) dt \quad (22)$$

where  $K_v$ ,  $K_p$ , and  $K_i \in \mathbb{R}^{(n-1) \times (n-1)}$  are the diagonal gain matrices.  $\mathbf{x}$  and  $\dot{\mathbf{x}}$  are the measured values of the position and velocity of the  $\mathbf{x}$  components.

$\ddot{x}_d$  calculated from (22) is substituted in  $\ddot{\mathbf{x}}$  of (20a) and (20b). If  $\mathbf{M}_p \mathbf{H}_p$  is not equal to zero, the torque  $\tau$  to realize  $\ddot{x}_d$  can be determined as

$$\tau = \{ \mathbf{M}_a - \mathbf{M}_a \mathbf{H}_p (\mathbf{M}_p \mathbf{H}_p)^{-1} \mathbf{M}_p \} (\mathbf{H}_a \ddot{x}_d - \mathbf{H} \dot{\mathbf{J}} \dot{\theta}) + \mathbf{b}_a - \mathbf{M}_a \mathbf{H}_p (\mathbf{M}_p \mathbf{H}_p)^{-1} \mathbf{b}_p. \quad (23)$$

When we apply torque  $\tau$  of (23) to the active joints, we will obtain the  $\mathbf{x}$  components acceleration of (22). The deviation of the manipulator from the desired path converges to zero asymptotically if  $K_v$ ,  $K_p$ , and  $K_i$  are chosen appropriately. As a result, the manipulator tracks the desired path.

Fig. 3 shows the path-tracking control system.

### B. Planning of Desired Path and Initial Conditions

As an initial condition, it is assumed that the manipulator is moving with sufficient initial velocity in the direction of the path when path-tracking control begins. This can be achieved, for example, by accelerating the active joints while the passive joint is fixed and then commencing the path-tracking control with the passive joint released.

The desired path should be planned geometrically so that the initial conditions can be realized by the active joints only. The manipulator has  $n - 1$  DOF when the passive joint is fixed. The initial angular velocity of the passive joint is zero. The initial position and direction of the desired path are limited by these conditions. On the other hand, the initial velocity along the path can be controlled arbitrarily by the active joints.

When path tracking is performed as part of point-to-point control, the passive joint should stop at an exact angle. The final direction of the path is also limited so that the angular velocity of the passive joint is zero.

### C. Velocity along Path

In this method, the  $s$  component is accelerated/decelerated in order to realize the desired value of the  $\mathbf{x}$  components. Therefore, the  $s$  component cannot be controlled directly. The time period necessary to travel along the path depends on the configuration of the path and the initial velocity along the path.

From (14),  $\mathbf{x}$  is constant when the manipulator moves along the desired path. Thus,  $\dot{\mathbf{x}} = \mathbf{0}$  and  $\ddot{\mathbf{x}} = \mathbf{0}$  on the path. Since  $\mathbf{H} \dot{\mathbf{J}} = -\dot{\mathbf{H}} \dot{\mathbf{J}}$ , acceleration along the path is

$$\ddot{s} = -(\mathbf{M}_p \mathbf{H}_p)^{-1} (\mathbf{M}_p \dot{\mathbf{H}}_p \dot{s} + \mathbf{b}_p) \quad (24)$$

from (20b). The initial value of  $s$  is  $s_0$ , and the final value is  $s_f$ . When initial values  $s_0$  and  $\dot{s}_0$  are given,  $s$  and  $\dot{s}$  can be calculated by numerical integration of (24) for  $s_0 \leq s \leq s_f$ . Thus, the time

trajectory of the manipulator is obtained. The final value of  $\dot{s}_f$  and the time period to travel along the path are also evaluated.

If the initial velocity along the path is too slow, the direction of  $\dot{s}$  may be inverted before reaching the final point, and the manipulator cannot complete path tracking. Therefore, it is desirable to estimate the minimum initial velocity necessary to reach the final point.  $\mathbf{M}_p$  and  $\mathbf{H}_p$  in (24) can be represented as functions of  $s$  only. On the path,  $\theta = \mathbf{H}_p \dot{s}$ . When the friction of the passive joint is negligibly small and  $\mathbf{b}_p$  is composed of Coriolis, centrifugal, and gravitational forces, (24) can be rewritten as

$$\ddot{s} = f(s) \dot{s}^2 + g(s) \quad (25)$$

where  $f(s)$  and  $g(s)$  are functions of  $s$  and do not depend on initial velocity  $\dot{s}_0$ . Note that

$$\ddot{s} = \frac{ds}{dt} \cdot \frac{d\dot{s}}{ds} = \frac{1}{2} \cdot \frac{d(\dot{s}^2)}{ds}. \quad (26)$$

Equation (25) is a linear differential equation with respect to  $\dot{s}^2$ . The solution of (25) is

$$\dot{s}^2(s) = \exp \left( \int_{s_0}^s 2f(\zeta) d\zeta \right) \cdot \left[ \dot{s}_0^2 + \int_{s_0}^s 2g(\zeta) \exp \left( - \int_{s_0}^{\zeta} 2f(\epsilon) d\epsilon \right) d\zeta \right]. \quad (27)$$

Since

$$\exp \left( \int_{s_0}^s 2f(\zeta) d\zeta \right) > 0$$

the condition for  $\dot{s}^2(s) > 0$  is

$$\dot{s}_0^2 > - \int_{s_0}^s 2g(\zeta) \cdot \exp \left( - \int_{s_0}^{\zeta} 2f(\epsilon) d\epsilon \right) d\zeta. \quad (28)$$

The right side of (28) is calculated by numerical integration. If  $\dot{s}_0$  is chosen so that  $\dot{s}_0^2$  is larger than the maximum of the integration value, the manipulator can reach the final point. It is clear from (28) that if  $g(s) \geq 0$  for  $s_0 \leq s \leq s_f$ , the manipulator can reach the final point for any  $\dot{s}_0 > 0$ .

The initial velocity necessary to reach the desired velocity at the final point or at a point halfway along the path can be calculated if the initial velocity is in excess of the minimum velocity. When (24) is integrated backward for  $s_0 \leq s \leq s_d$  with  $s$  and  $\dot{s}$  given final values  $s_d$  and  $\dot{s}_d$ , the initial velocity  $\dot{s}_0$  to realize the desired velocity  $\dot{s}_d$  is derived.

During real-time control,

$$\lambda = \frac{s - s_0}{s_f - s_0} \quad (29)$$

and  $0 < \lambda < 1$  on the path. The value of  $\lambda$  is monitored while the manipulator is tracking the path. The control terminates when  $\lambda > 1$ .

### D. Control of a Manipulator and Multiple Passive Joints

A manipulator composed of  $n - 1$  active joints and one passive joint is considered in Sections IV-A to IV-C. However, the proposed control method is easily extended to a manipulator with multiple passive joints. In  $n$ -dimensional operational space, it is necessary to control  $n - 1$  components to keep the manipulator on the desired path. Therefore,  $n - 1$  active joints are necessary. The manipulator is assumed to have  $m > 1$  passive joints. In this case, the manipulator is redundant in operational space, and the extended Jacobian method in path coordinate space is applied. The equation of motion is

$$\mathbf{M}(\theta) \ddot{\theta} + \mathbf{b}(\theta, \dot{\theta}) = \mathbf{u} \quad (30)$$

$$\mathbf{u} = [\tau^T \quad \mathbf{0}]^T \quad (31)$$

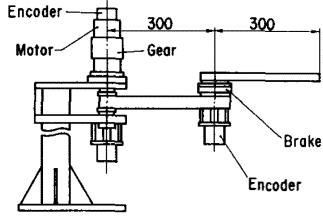


Fig. 4. Two-degree-of-freedom manipulator.

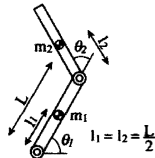


Fig. 5. Model of the manipulator.

where  $\theta \in \mathbb{R}^{n+m-1}$ ,  $M(\theta) \in \mathbb{R}^{(n+m-1) \times (n+m-1)}$ ,  $b(\theta, \dot{\theta}) \in \mathbb{R}^{n+m-1}$ ,  $u \in \mathbb{R}^{n+m-1}$ , and  $\tau \in \mathbb{R}^{n-1}$ .

Here,  $m-1$  auxiliary components,  $z_1, \dots, z_{m-1}$ , are added to the path coordinates  $p$ .

$$\begin{aligned} p &= [x_1, \dots, x_{n-1}, s, z_1, \dots, z_{m-1}] \\ &= [x^T, y^T]^T \end{aligned} \quad (32)$$

where  $x \in \mathbb{R}^{n-1}$  and  $y \in \mathbb{R}^m$ . All the components of  $p$  including the auxiliary components should be independent, and the Jacobian matrix  $J \in \mathbb{R}^{(n+m-1) \times (n+m-1)}$  should be nonsingular. The equation of motion is partitioned as

$$M_a H_a \ddot{x} + M_a H_p \ddot{y} - M_a H \dot{J} \dot{\theta} + b_a = \tau \quad (33a)$$

$$M_p H_a \ddot{x} + M_p H_p \ddot{y} - M_p H \dot{J} \dot{\theta} + b_p = 0. \quad (33b)$$

If matrix  $M_p H_p \in \mathbb{R}^{m \times m}$  is nonsingular,

$$\ddot{y} = (M_p H_p)^{-1} (-M_p H_a \ddot{x} + M_p H \dot{J} \dot{\theta} - b_p). \quad (34)$$

The control law is a combination of PID feedback in (22) and the torque computation

$$\begin{aligned} \tau &= \{M_a - M_a H_p (M_p H_p)^{-1} M_p\} (H_a \ddot{x} - H \dot{J} \dot{\theta}) \\ &\quad + b_a - M_a H_p (M_p H_p)^{-1} b_p. \end{aligned} \quad (35)$$

It has almost the same form as (23).

## V. EXPERIMENTS

### A. Two-Degree-of-Freedom Manipulator

We conducted experiments using these control methods with a 2-DOF horizontally articulated manipulator. Fig. 4 shows the manipulator. The first axis ( $\theta_1$ ) is a active joint and the second axis ( $\theta_2$ ) is a passive joint. The active joint is driven by a dc servo motor with a harmonic-drive gear. The brake of the passive joint is electromagnetic. Fig. 5 shows the model of the manipulator. Table I shows the parameters of the model.  $M$  and  $b$  in (1) are defined in (36), found at the bottom of the following page.

### B. Control in Cartesian Space

The control scheme of Section II is demonstrated first. Cartesian space is used as operational space. The origin is at the first joint.

TABLE I  
PARAMETERS OF THE MANIPULATOR

$m_1$	Mass of link 1	2.0 kg
$m_2$	Mass of link 2	1.0 kg
$L$	Length of links 1 and 2	0.3 m
$D_1$	Viscous friction of the actuator	2.2 N·m·s/rad
$J_M$	Moment of inertia of the actuator	0.24 kgm <sup>2</sup>

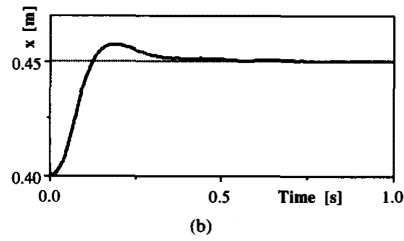
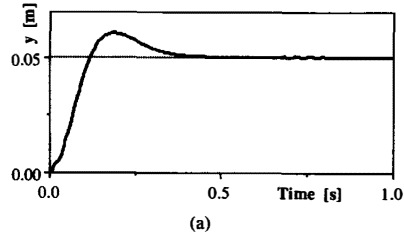


Fig. 6. Step response of the active component. (a) Active component:  $y$ . (b) Active component:  $x$ .

The coordinate transformation from joint space to operational space is represented as

$$\begin{aligned} x &= L \cos \theta_1 + L \cos(\theta_1 + \theta_2) \\ y &= L \sin \theta_1 + L \sin(\theta_1 + \theta_2). \end{aligned} \quad (37)$$

The Jacobian matrix is

$$J = L \begin{bmatrix} -\sin \theta_1 - \sin(\theta_1 + \theta_2) & -\sin(\theta_1 + \theta_2) \\ \cos \theta_1 + \cos(\theta_1 + \theta_2) & \cos(\theta_1 + \theta_2) \end{bmatrix}. \quad (38)$$

There are two cases: the case in which  $y$  is the active component and  $x$  is the passive component, and the case in which  $x$  is the active component and  $y$  is the passive component. From the state where the manipulator is at rest, a step change of the reference is given for the active component in each case. Fig. 6 shows the response. The initial position is  $x = 0.4$ (m),  $y = 0$ (m). In Fig. 6(a),  $y$  is the active component and the reference is  $y = 0.05$ (m). In Fig. 6(b)  $x$  is the active component and the reference is  $x = 0.45$ (m). The feedback gains are set so that the pole of the system is a triple root. The sampling interval is 2 ms with a 16-MHz i80386 + 80387 CPU. (In the case of multiple degrees of freedom, (11) requires  $[n^3 - 2n^2r + nr^2 + 7n^2 - 3nr + 2r^2]$  multiplications and the inversion of a  $(n-r) \times (n-r)$  matrix. It would be desirable to develop an efficient computation algorithm.) In the experimental result, the measured value of the active component (solid line) converges to the reference (dotted line). The error from the reference after the convergence is 0.14 mm in Fig. 6(a) and 0.08 mm in Fig. 6(b). Next, a desired trajectory is assigned for the active component. Fig. 7 shows the result of the trajectory tracking. The active component increases with constant velocity from the stationary state and decreases with constant velocity in the desired trajectory. An abrupt change in velocity occurs at the beginning of the trajectory and at the moment the direction changes. The measured value (solid line) follows the

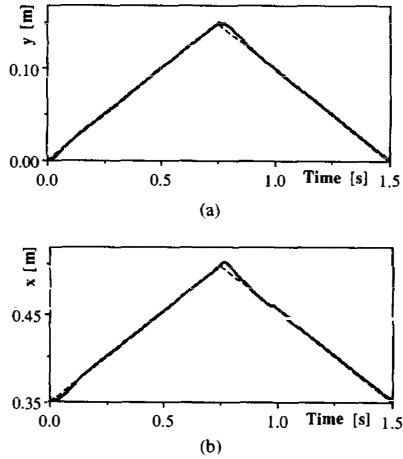


Fig. 7. Tracking of a desired trajectory. (a) Active component:  $y$ . (b) Active component:  $x$ .

desired trajectory (dotted line) except just after those moments. The stick diagram (Fig. 8) represents the motion of the manipulator when the  $y$  component tracks a desired trajectory with constant velocity. The initial acceleration is done with the passive joint fixed. In Fig. 8, the  $y$  component increases constantly.

### C. Dynamic Singularity

In the dynamic singular point, discussed in Section II-D, it is difficult to apply the proposed control method. In the case of a 2-DOF manipulator, the condition of dynamic singularity is  $\mathbf{M}_p \mathbf{H}_p = 0$ . Fig. 9 shows the dynamic singular points of the manipulator used in the experiments.  $\mathbf{M}_p \mathbf{H}_p = 0$  at these points. It is necessary to avoid these points in the control. In Fig. 9(a),  $y$  is the active component, and in Fig. 9(b),  $x$  is the active component. The dynamic singular points of Fig. 9(a) are not coincident with those of Fig. 9(b). In other words, where one component is not controllable, the other component is.

### D. Modeling Error

This method depends essentially on the dynamic model of the manipulator. In the experiments of this paper, each parameter of the manipulator was calculated or determined experimentally in advance. However, a load at the tip of the manipulator causes a change in the dynamic parameters.

The control of the active components in the proposed method has basically the same form as the computed torque method. In other words, the control of the active components is no less robust than the computed torque method of a conventional manipulator having an actuator for each joint. A high-gain feedback can suppress the error caused by the modeling error if the change of the model is not so large.

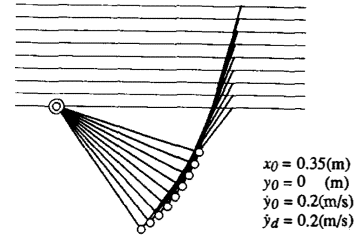


Fig. 8. Motion of the manipulator.

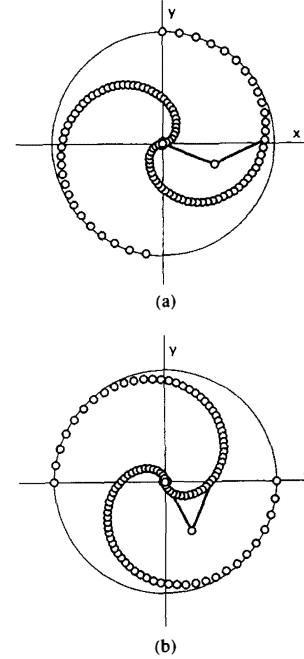


Fig. 9. Location of dynamic singular points. (a) Active component:  $y$ . (b) Active component:  $x$ .

On the other hand, the passive components absorb the modeling error. If the motion of the manipulator is simulated in advance, the trajectory of passive components deviates from the simulation. In path-tracking control, the velocity profile along the path changes. The proposed method is sensitive to the modeling error in this sense. The authors expect that this method may become more effective if it is used together with a real-time parameter identification or an adaptive control method.

We also investigated the robustness of the control method experimentally. A weight (0.5 kg) is attached to the tip of the manipulator. The same step-response experiments as in Fig. 6 are done using

$$\mathbf{M} = \begin{bmatrix} \frac{1}{3}m_1L^2 + \frac{4}{3}m_2L^2 + m_2L^2 \cos \theta_2 + J_M & \frac{1}{3}m_2L^2 + \frac{1}{2}m_2L^2 \cos \theta_2 \\ \frac{1}{3}m_2L^2 + \frac{1}{2}m_2L^2 \cos \theta_2 & \frac{1}{3}m_2L^2 \end{bmatrix}$$

$$\mathbf{b} = \begin{bmatrix} -m_2L^2 \sin \theta_2 \dot{\theta}_1 \dot{\theta}_2 - \frac{1}{2}m_2L^2 \sin \theta_2 \dot{\theta}_2^2 + D_1 \dot{\theta}_1 \\ \frac{1}{2}m_2L^2 \sin \theta_2 \dot{\theta}_1^2 \end{bmatrix}. \quad (36)$$

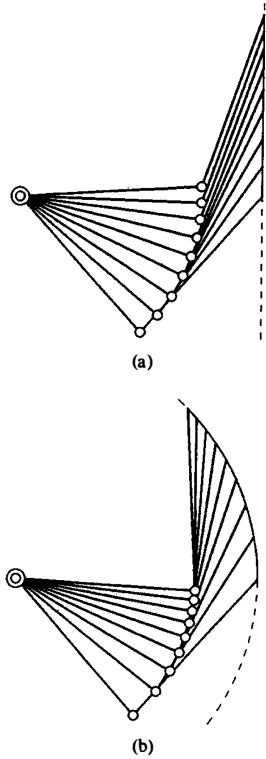


Fig. 10. Path tracking motion. (a) Straight line path. (b) Circular arc path.

parameters without considering the weight. The error of the active components after the step response is  $x : 0.18$  mm,  $y : 0.24$  mm. The increase in the error of the active component caused by the modeling error is small.

#### E. Path Tracking Control

The path-tracking control scheme of Section IV is applied to the manipulator. In this manipulator, the initial direction of the desired path should be tangential to a circle centered at the first axis. First the passive joint is fixed and the active joint is accelerated. Path tracking begins when the brake is released. The desired path of Figs. 10(a) and 11(a) is given as a straight line. In the case of (a), the path coordinate space is Cartesian space. The coordinate transformation is (37), and the Jacobian matrix (38). The desired path (a) is represented as  $x_d = 0.4$ (m). The desired path of Figs. 10(b) and 11(b) is given as a circular arc around the first axis. In the case of (b), the path coordinate space is a polar coordinate space whose origin is at the first joint.

$$\mathbf{p} = [r, \phi]^T, \quad r = 2L \cos \frac{\theta_2}{2}, \quad \phi = \theta_1 + \frac{\theta_2}{2}. \quad (39)$$

The Jacobian matrix is

$$\mathbf{J} = L \begin{bmatrix} 0 & -L \sin \frac{\theta_2}{2} \\ 1 & \frac{1}{2} \end{bmatrix}. \quad (40)$$

The desired path is  $r_d = 0.4$ (m). Fig. 10 illustrates the results of the path-tracking control experiments. The initial condition is  $y_0 = 0$  m,  $\dot{y}_0 = 0.7$  m/s in both cases. The results (solid lines) follow the desired paths (dotted lines). Trackings to the different paths are achieved from

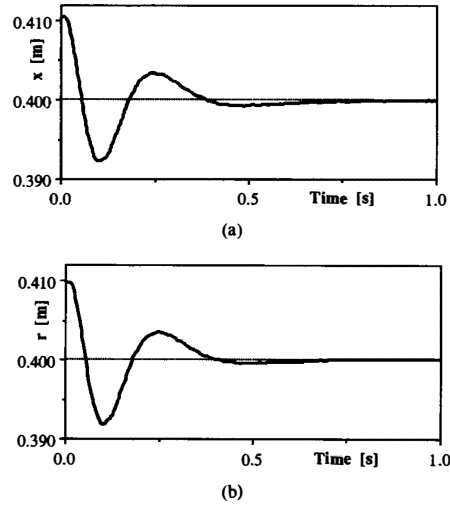


Fig. 11. Suppression of tracking error. (a) Straight line path. (b) Circular arc path.

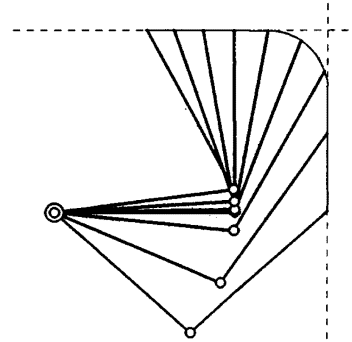


Fig. 12. Tracking of a composite path.

the same initial condition. The maximum deviation is 0.29 mm in Fig. 10(a), and 0.72 mm in Fig. 10(b). Fig. 11 shows the response when the initial position is not on the path. The deviations converge to zero by means of the feedback control. Fig. 12 shows tracking of a path that includes straight and circular path segments. In this way, a complicated path can be composed of several simple path segments.

#### VI. CONCLUSIONS

A method to control a manipulator with passive joints in operational space has been proposed. The equation of motion is represented in terms of operational coordinates. The desired acceleration can be generated at active components equal in number to the active joints by using dynamic coupling among the coordinates. This method is extended to path-tracking control. A *path coordinate system* based on the desired path is defined. The equation of motion of the manipulator is described in terms of the path coordinates. The acceleration of the components normal to the desired path is controlled using the dynamic coupling among components. This in turn keeps the manipulator on the desired path. The effectiveness of the method was verified by experiments using a 2-DOF manipulator with a passive joint. One of the two coordinates in Cartesian space is controlled to follow a desired value. The experiments also showed that the

path of the manipulator can be controlled precisely by use of the proposed method. Since this method uses closed-loop control, precise tracking is possible in the presence of disturbances. The path of the manipulator can be prescribed with this method and it may be combined with obstacle avoidance or other path-planning algorithms.

## ACKNOWLEDGMENT

The authors would like to express their appreciation to Dr. N. Oyama, Director of the Robotics Department, Mechanical Engineering Laboratory, for his constant support. They would also like to thank the members of the Biorobotics Division and the Cybernetics Division, MEL, and K. Lynch, Carnegie Mellon University, for their assistance.

## REFERENCES

- [1] S. Hirose and Y. Umetani, "The development of soft gripper for the versatile robot hand," in *Proc. 7th ISIR*, 1977, pp. 353-360.
- [2] J. Y. S. Luh, M. W. Walker, and R. P. Paul, "Resolved acceleration control of mechanical manipulators," *IEEE Trans. Automat. Contr.*, vol. 25, no. 3, pp. 468-474, 1980.
- [3] K. D. Young, "Controller design for a manipulator using theory of variable structure systems," *IEEE Trans. Syst. Man Cybern.*, vol. SMC-8, no. 2, pp. 101-109, 1978.
- [4] E. Freund, "Fast nonlinear control with arbitrary pole-placement for industrial robots and manipulators," *Int. J. Robotics Res.*, vol. 1, no. 1, pp. 65-78, 1982.
- [5] K. Youcef-Toumi and H. Asada, "The design of open-loop manipulator arms with decoupled and configuration-invariant inertia tensors," in *Proc. IEEE Int. Conf. Robotics Automat.*, 1986, pp. 2018-2026.
- [6] B. Boravac, M. Vukobratović, and D. Surla, "An approach to biped control synthesis," *Robotica*, vol. 7, no. 3, pp. 231-241, 1989.
- [7] T. Arai and S. Chiu, "Control of robot using coupled torque between joints," in *Proc. IEEE Int. Workshop Intell. Robots Syst. (IROS'90)*, 1990, pp. 963-968.
- [8] H. Arai and S. Tachi, "Position control of a manipulator with passive joints using dynamic coupling," *IEEE Trans. Robotics Automat.*, vol. 7, no. 4, pp. 528-534, 1991.
- [9] —, "Position control system of a two degree of freedom manipulator with a passive joint," *IEEE Trans. Ind. Electron.*, vol. 38, no. 1, pp. 15-20, 1991.
- [10] A. Jain and G. Rodriguez, "Kinematics and dynamics of under-actuated manipulators," in *Proc. IEEE Int. Conf. Robotics Automat.*, 1991, pp. 1754-1759.
- [11] E. Papadopoulos and S. Dubowsky, "Failure recovery control for space robotic systems," in *Proc. 1991 Amer. Contr. Conf.*
- [12] J. Baillieul, "Kinematic programming alternatives for redundant manipulators," in *Proc. IEEE Int. Conf. Robotics Automat.*, 1985, pp. 722-728.
- [13] K. G. Shin and N. D. McKay, "Minimum-time control of robotic manipulators with geometric path constraints," *IEEE Trans. Automat. Contr.*, vol. 30, no. 6, pp. 531-541, 1985.
- [14] J. E. Bobrow, S. Dubowsky and J. S. Gibson, "On the optimal control of robotic manipulators along specified paths," *Int. J. Robot. Res.*, vol. 4, no. 3, pp. 3-17, 1985.
- [15] F. Pfeiffer and R. Johanni, "A concept for manipulator trajectory control," *IEEE J. Robotics Automat.*, vol. RA-3, no. 3, pp. 115-123, 1987.

## Bounds on the Largest Singular Value of the Manipulator Jacobian

Inge Spangelo, J. Richard Saggi, and Olav Egeland

**Abstract**—In this work, we prove that if the manipulator Jacobian is properly scaled, the largest singular value is bounded within a small interval close to unity. In this case, the inverse of the smallest singular value is a good estimate of the condition number. This is useful in singularity analysis. Bounds are derived for a general six-joint manipulator and for the ABB IRB 2000 industrial robot in a case study.

## I. INTRODUCTION

The damped least-squares solution has been proposed for inverse kinematics with singularity robustness [1], [2]. A critical point in the implementation of this method is the selection of an appropriate damping factor that gives a good compromise between accuracy and feasibility of the solution.

Nakamura and Hanafusa [1] proposed computing the damping factor from the manipulability. Far from singularities, the damping factor was set to zero, while a nonzero damping factor was used close to singularities where the manipulability approaches zero. Maciejewski and Klein [3] proposed computing the damping factor as a function of the smallest singular value of the Jacobian. They commented that the largest singular value of the Jacobian was approximately unity if the Jacobian was appropriately scaled. This observation was also made by Wampler [2] who stated that the Jacobian should be scaled with the maximum reach of the arm. The 2-norm condition number of the Jacobian is the ratio between the largest and the smallest singular values. If it can be proved that the largest singular value is close to unity, it follows that the inverse of the smallest singular value is a good estimate of the condition number.

The main contribution of this paper is the proof that the largest singular value is bounded close to unity when the Jacobian is properly scaled. We derive bounds for the largest singular value of the manipulator Jacobian and discuss the effect of scaling the translations. It is shown that if the translations are properly scaled, the largest singular value is bounded within a small interval slightly larger than unity. The analysis is done for a general six-joint manipulator, and for the ABB IRB 2000 industrial robot.

## II. BACKGROUND

The six-dimensional vector of joint coordinates is denoted  $\mathbf{q}$ . The three-dimensional vector of end effector velocity is denoted  $\mathbf{v}$ , while the three-dimensional angular velocity vector is denoted  $\boldsymbol{\omega}$ . The  $6 \times 6$  Jacobian matrix  $\mathbf{J}$  is defined by

$$\begin{bmatrix} \mathbf{v} \\ \boldsymbol{\omega} \end{bmatrix} = \mathbf{J}(\mathbf{q})\dot{\mathbf{q}}. \quad (1)$$

This matrix was termed the partial velocity matrix by Wampler [2]. If  $\mathbf{J}$  is full rank,  $\dot{\mathbf{q}}$  can be found from (1) by Gaussian elimination. In singular configurations, a solution will only exist if  $(\mathbf{v}^T \boldsymbol{\omega}^T)^T \in$

Manuscript received November 25, 1991; revised June 1, 1992. This work was supported by the Royal Norwegian Council for Scientific and Industrial Research through the Center for Robotics Research at the Norwegian Institute of Technology and by ABB Robotics.

The authors are with the Division of Engineering Cybernetics, The Norwegian Institute of Technology, N-7034 Trondheim, Norway.

IEEE Log Number 9205082.